THE PROTEIN SOCIETY

The molecular architecture of QdtA, a sugar 3,4-ketoisomerase from *Thermoanaerobacterium thermosaccharolyticum*

James B. Thoden and Hazel M. Holden*

Department of Biochemistry, University of Wisconsin, Madison, Wisconsin 53706

Received 31 January 2014; Revised 1 March 2014; Accepted 3 March 2014
DOI: 10.1002/pro.2451
Published online 10 March 2014 proteinscience.org

Abstract: Unusual di- and trideoxysugars are often found on the O-antigens of Gram-negative bacteria, on the S-layers of Gram-positive bacteria, and on various natural products. One such sugar is 3-acetamido-3,6-dideoxy-D-glucose. A key step in its biosynthesis, catalyzed by a 3,4-ketoisomerase, is the conversion of thymidine diphosphate (dTDP)−4-keto-6-deoxyglucose to dTDP-3-keto-6-deoxyglucose. Here we report an X-ray analysis of a 3,4-ketoisomerase from *Thermoanaerobacterium thermosaccharolyticum*. For this investigation, the wild-type enzyme, referred to as QdtA, was crystallized in the presence of dTDP and its structure solved to 2.0-Å resolution. The dimeric enzyme adopts a three-dimensional architecture that is characteristic for proteins belonging to the cupin superfamily. In order to trap the dTDP-4-keto-6-deoxyglucose substrate into the active site, a mutant protein, H51N, was subsequently constructed, and the structure of this protein in complex with the dTDP–sugar ligand was solved to 1.9-Å resolution. Taken together, the structures suggest that His 51 serves as a catalytic base, that Tyr 37 likely functions as a catalytic acid, and that His 53 provides a proton shuttle between the C-3′ hydroxyl and the C-4′ keto group of the hexose. This study reports the first three-dimensional structure of a 3,4-ketoisomerase in complex with its dTDP–sugar substrate and thus sheds new molecular insight into this fascinating class of enzymes.

Keywords: dideoxysugar; 3,4-ketoisomerase; cupin superfamily; enzyme mechanism; O-antigen; S-layer; 3-acetamido-3,6-dideoxy-D-glucose; protein structure

Introduction

The bacterial 3,4-ketoisomerases play key roles in the production of unusual 3,6-dideoxysugars such as 3-acetamido-3,6-dideoxy-D-galactose (Fuc3NAc), 3-acetamido-3,6-dideoxy-D-glucose (Qui3NAc), and D-mycaminose (Scheme 1). The first two sugars, 3-acetamido-3,6-dideoxy-D-galactose and 3-acetamideo-3,6-dideoxy-D-glucose, have been observed in the S-layer of *Aneurinibacillus thermoaerophilus* and *Thermoanaerobacterium thermosaccharolyticum*, respectively, and have also been identified on the lipopolysaccharides of several Gram-negative bacteria.[1–6] The third sugar, D-mycaminose, is found attached to a variety of macrolide rings including tylosin, an antibiotic produced by *Streptomyces fradiae*.[7]

The complete biosynthetic pathways for the production of 3-acetamido-3,6-dideoxy-D-galactose and 3-acetamido-3,6-dideoxy-D-glucose were first reported by the Messner laboratory in 2003 and 2008, respectively, and are shown in Scheme 2.[1,2] As

Abbreviations: dTDP, thymidine diphosphate; HEPPS, *N*-2-hydroxyethylpiperazine-*N*′-3-propanesulfonic acid; HPLC, high-performance liquid chromatography; PCR, polymerase chain reaction.

X-ray coordinates have been deposited in the Research Collaboratory for Structural Bioinformatics, Rutgers University, New Brunswick, NJ (accession nos. 4O9E and 4O9G).

Grant sponsor: NIH (to HMH); Grant number: DK47814.

*Correspondence to: Hazel M. Holden, Department of Biochemistry, University of Wisconsin, Madison, WI 53706. E-mail: Hazel_Holden@biochem.wisc.edu

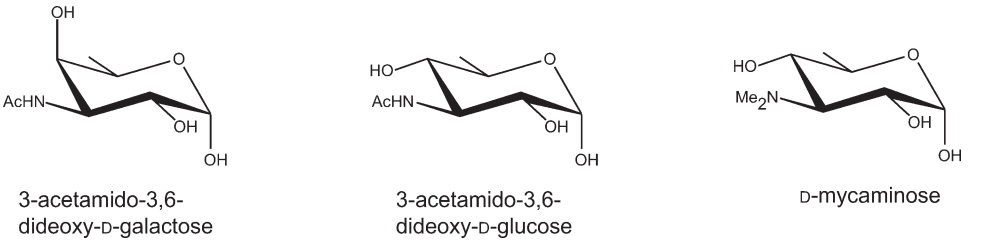

Scheme 1. Examples of 3,6-dideoxysugars.

can be seen, the 3,4-ketoisomerases (QdtA or FdtA) catalyze the third steps in the pathways. Whereas both QdtA and FdtA function on the same substrate [thymidine diphosphate (dTDP)−4-keto-6-deoxyglucose], the products of their reactions differ with respect to the orientations of the hydroxyl groups about the hexose C-4′ carbons. Specifically, QdtA functions as a retaining enzyme whereas FdtA inverts the configuration about the C-4′ carbon.

In 2007, our laboratory determined the first structure of a sugar 3,4-ketoisomerase, namely that of FdtA from *A. thermoaerophilus*.[8] Each subunit of the dimeric enzyme is characterized by a β-barrel motif with one α-helix. A cluster of three histidine residues lines the active site region, two of which appear to be strictly conserved amongst the 3,4-ketoisomerases. Subsequent site-directed mutagenesis experiments suggested that one of these histidines, His 49, functions as an active site base. Whereas this X-ray analysis of a 3,4-ketoisomerase revealed the overall fold of the enzyme, the study was somewhat limited because it was never possible to determine the structure of FdtA with a bound dTDP–sugar substrate or analog.

Here we report the molecular architecture of QdtA from *T. thermosaccharolyticum*. For this investigation, crystals were grown of both the wild-type enzyme in complex with dTDP and of a site-directed mutant protein (H51N) in complex with dTDP-4-keto-6-deoxyglucose. The structures reveal that His 51 is located in an ideal position to serve as the catalytic base, that Tyr 37 likely functions as the active site acid, and that His 53 is correctly situated to function as a proton shuttle between the C-3′ hydroxyl group and the C′-4 keto functionality. The investigation described herein provides additional insight into the sugar 3,4-ketoisomerases.

Results and Discussion

Biochemical analysis of T. thermosaccharolyticum QdtA

The amino acid sequence of the *T. thermosaccharolyticum* QdtA utilized in this investigation differs from that deposited in GenBank (A52S, F94L, L95V, and C116Y). Amino acid sequence alignments with other QdtA (or putative QdtA) enzymes demonstrate that Position 52 is either an alanine or serine, Positions 94 and 95 show variability, and Position 116 is always a tyrosine rather than a cysteine. In the model described here, Ser 52 is ∼7 Å and Leu 94 and Val 95 are over 10 Å from the active site. Importantly, Tyr 116, as described below, forms a stacking interaction with the thymine ring of the dTDP–sugar substrate.

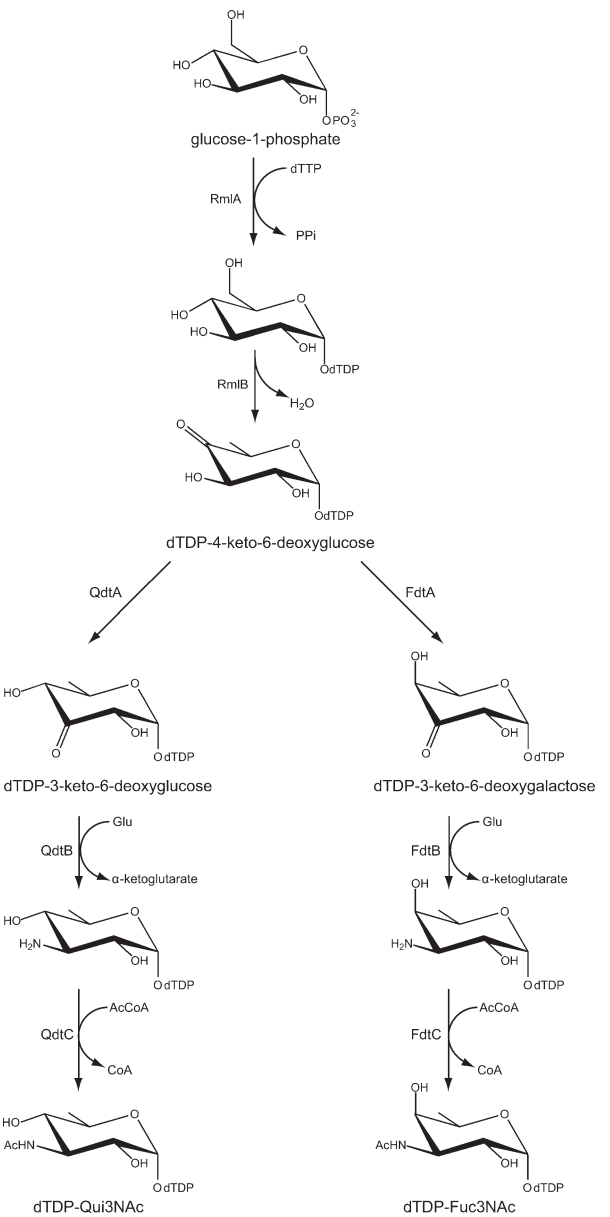

Scheme 2. Biosynthetic pathway for the production of dTDP-Qui3NAc and dTDP-Fuc3NAc.

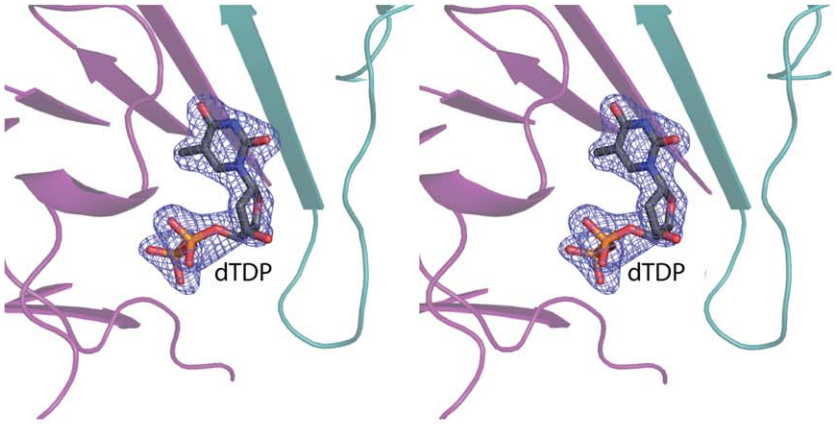

(a)

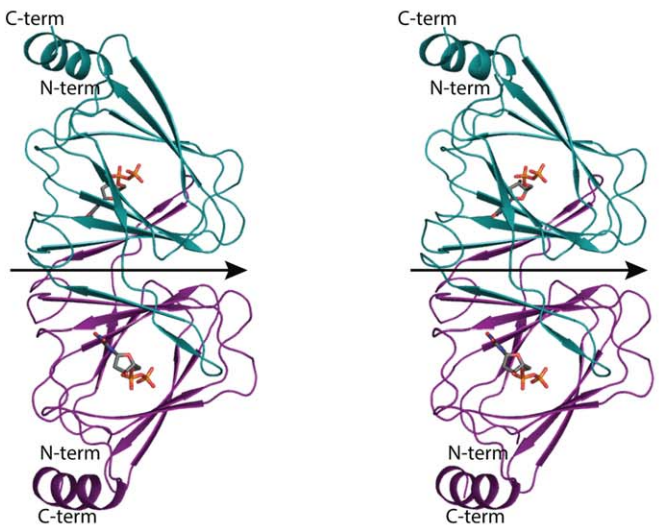

(b)

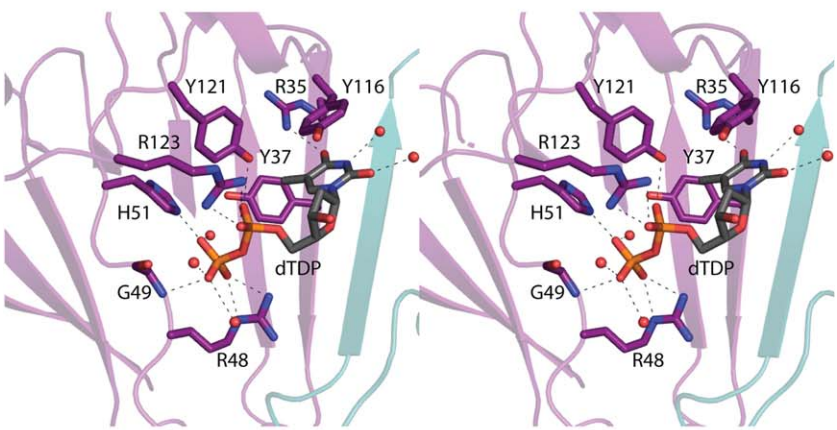

(c)

Figure 1. The three-dimensional architecture of QdtA. The structure of QdtA was solved in the presence of dTDP. Shown in (a) is the electron density corresponding to the bound ligand in Subunit 1 of the dimer. The map was calculated with coefficients of the form $F_o - F_c$, where F_o was the native structure factor amplitude and F_c was the calculated structure factor amplitude. The map was contoured at 4σ. The ligand was not included in the map calculation or in the model refinement. A ribbon representation of the QdtA dimer is displayed in (b) with Subunits 1 and 2 depicted in purple and teal, respectively. The arrow indicates the position of the twofold rotational axis that relates the two subunits. The N- and C-termini are located at ~12 Å from each other. A close-up stereo view of the region surrounding the dTDP ligand in Subunit 1 is presented in (c). The dashed lines indicate potential hydrogen bonds. Ordered water molecules are depicted as red spheres. All figures were created using PyMOL.[19]

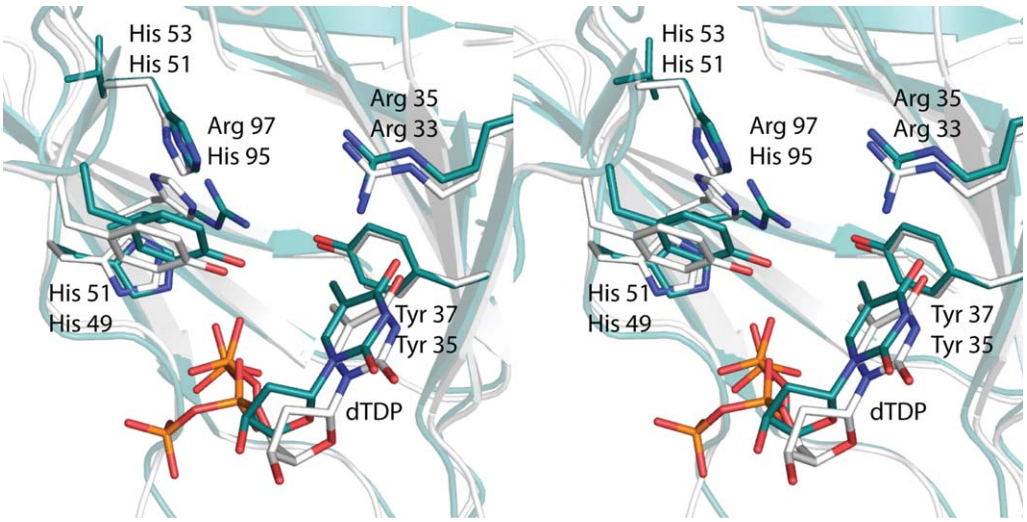

Figure 2. Comparison of the QdtA and FdtA active sites. Those amino acid residues corresponding to QdtA and FdtA are displayed in teal and white, respectively. The top labels refer to QdtA residues whereas the bottom labels correspond to FdtA residues.

The version of *T. thermosaccharolyticum* QdtA described here is fully functional. Indeed, a kinetic analysis showed that the K_m for dTDP-4-keto-6-deoxyglucose is 0.32 ± 0.04 mM and the k_{cat} is 2.8 ± 0.3 s^{-1}. The overall catalytic efficiency of QdtA is 8.8 x 10^3 M^{-1} s^{-1}.

Structure of the wild-type T. thermosaccharolyticum QdtA

The QdtA/dTDP complex crystals grew from pentaerythritol propoxylate (pH 8.0) and contained one dimer in the asymmetric unit. The structure was solved and refined to 2.0-Å resolution. Shown in Figure 1(a) is the electron density corresponding to the bound dTDP ligand in Subunit 1. Overall the quality of the electron density for both subunits in the asymmetric unit was excellent with no breaks in the polypeptide chain backbones from Met 1 to Phe 136. Interestingly, there was electron density positioned on a crystallographic dyad that corresponded to one molecule of tetraerythritol propoxylate, a contaminant of pentaerythritol propoxylate.

A ribbon representation of the QdtA dimer is displayed in Figure 1(b). The molecular architecture of QdtA places it into the well-characterized cupin superfamily.[9–11] Members of this superfamily include both metal-dependent and metal-independent enzymes as well as seed storage and sugar-binding proteins. Each subunit of the dimer consists of 11 β-strands and a C-terminal α-helix. The N- and C-termini are separated by ~12 Å. The β-strands form an antiparallel flattened β-barrel that can be envisioned as two layers of four and seven β-strands, respectively. Classical domain swapping occurs as the second and third β-strands from one subunit form part of the seven-stranded β-sheet in the second subunit. In light of the fact that the α-carbons for the two subunits superimpose with a root-mean-square deviation of 0.19 Å, the following discussion refers only to Subunit 1 in the X-ray coordinate file.

A close-up view of the dTDP-binding site is presented in Figure 1(c). The thymine ring lies within hydrogen bonding distance to the guanidinium group of Arg 35 and two water molecules. In addition, Tyr 31 and Tyr 116 form T-shaped and parallel stacking interactions, respectively, with the thymine ring. The pyrophosphoryl group of the ligand hydrogen bonds with the backbone amide group of Gly 49, the side chains of Arg 48 His 51, Tyr 121, and Arg 123, and three water molecules.

As noted in the Introduction, the first structural model of a sugar 3,4-ketoisomerase to be reported was that of FdtA from *A. thermoaerophilus*.[8] FdtA and QdtA demonstrate an amino acid sequence identity of 55% and a sequence similarity of 68%. Not surprisingly, the two enzymes superimpose with a root-mean-square deviation of 0.90 Å for 125 α-carbons. A superposition of the active site regions for QdtA and FdtA is presented in Figure 2. The dTDP ligands adopt slightly different conformations. In QdtA the pyrophosphoryl group is directed toward the interior of the protein whereas in FdtA it projects outward. Overall the active sites are similar with the only major difference being the replacement of His 95 in FdtA with Arg 97 in QdtA. This difference may play a role in determining the overall stereochemical outcome of the dTDP-product as discussed below.

Structure of the H51N mutant protein of T. thermosaccharolyticum *QdtA*

Previous site-directed mutagenesis experiments implicated His 49 in FdtA as the catalytic base that initiates catalysis by abstracting the C-3′ proton from the sugar.[8] This residue is structurally conserved in QdtA as His 51 (Fig. 2). Thus, in an attempt to prepare a QdtA/dTDP–sugar complex,

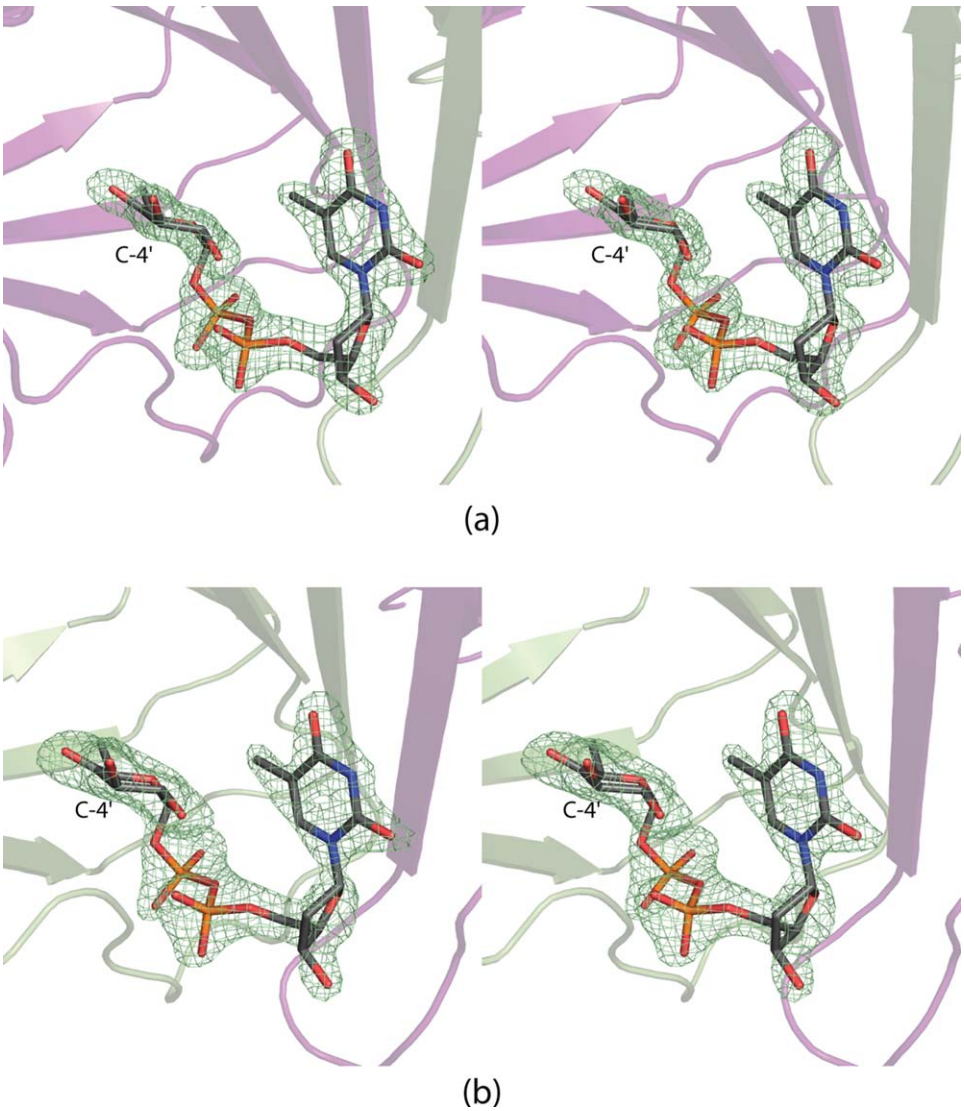

Figure 3. Electron density for the dTDP–sugars. The electron density maps shown in (a) and (b) correspond to the dTDP–sugar ligands found in the active sites of Subunits 1 and 2, respectively. The maps, contoured at 4σ, were calculated with coefficients of the form $F_o - F_c$, where F_o was the native structure factor amplitude and F_c was the calculated structure factor amplitude. The ligands were not included in the map calculations or in the initial model refinements.

the H51N site-directed mutant protein was subsequently prepared and shown to be catalytically inactive. Its three-dimensional structure was analyzed in the presence of the substrate, dTDP-4-keto-6-deoxyglucose (Scheme 2). The model was refined to a nominal resolution of 1.9 Å. The electron densities corresponding to the bound dTDP–sugars in Subunits 1 and 2 of the dimer are presented in Figure 3(a,b), respectively. In both subunits, the electron density corresponding to the C-4′ position of the pyranosyl moiety demonstrates that the keto-form of the sugar, with sp^2 hybridization, has been trapped within the active site cleft.

Overall the polypeptide chains for the wild-type QdtA and the H51N mutant protein are similar such that their α-carbons superimpose with a root-mean-square deviation of 0.18 Å. Only two amino acid residues change position significantly upon dTDP–sugar binding [Fig. 4(a)]. Specifically, the side chain of Arg 97 shifts in the active site to accommodate the C-4′ keto group of the dTDP–sugar. Likewise, the side chain of Gln 58 reorients such that Nε2 lies within 2.5 Å to Oη of Tyr 37. In the wild-type enzyme/dTDP complex model, this distance is 3.7 Å. A close-up view of the active site in Subunit 1 is provided in Figure 4(b). The interactions between the protein and the thymine ring, the deoxyribose, and the pyrophosphoryl group of the dTDP–sugar are virtually identical to those observed for the wild-type enzyme with bound dTDP. Key residues that anchor the pyranosyl group of the dTDP–sugar to the protein include His 53 and Arg 97.

Implications for the catalytic mechanism

As can be seen in Figure 4(a), substituting an asparagine for a histidine residue at Position 51 resulted in

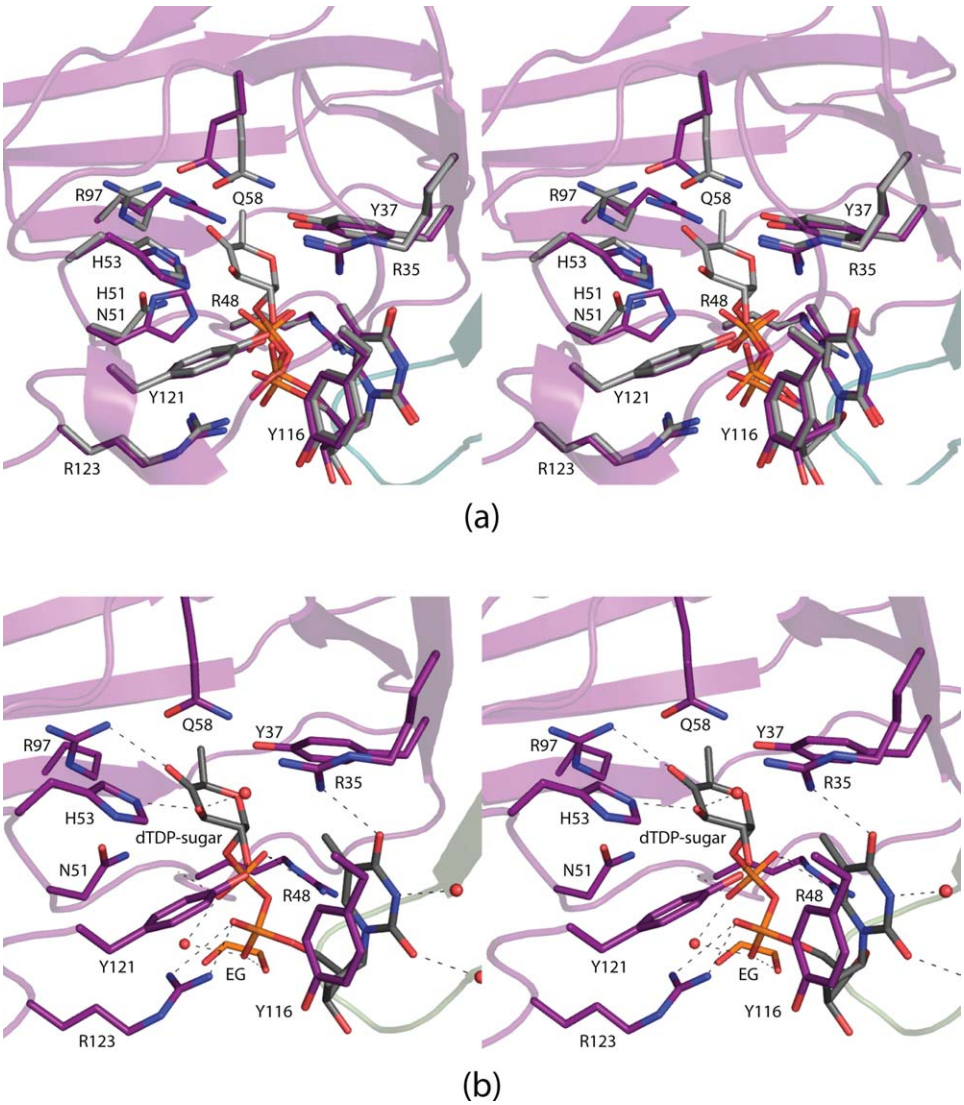

Figure 4. Active site of the H51N mutant protein. Shown in (a) is a superposition of the active site of the H51N mutant protein (gray bonds) onto that of the wild-type enzyme (purple bonds). Only two residues, Gln 58 and Arg 97, shift significantly upon binding the dTDP–sugar ligand. The hydrogen-bonding pattern surrounding the dTDP–sugar substrate in the H51N mutant protein is displayed in (b). The dashed lines indicate distances of 3.2 Å or shorter. An ethylene glycol molecule, labeled EG, was observed binding near the pyrophosphoryl group of the ligand.

little three-dimensional perturbation of the surrounding region. Thus, by combining the two structures described in this investigation, it is possible to obtain a reasonable model for the Michaelis complex as depicted in Figure 5. In this model, His 51 lies within ~4 Å of the C-3′ carbon. Tyr 37, situated on the opposite side of the pyranosyl ring, is positioned within 3.2 Å from the C-4′ carbon. The imidazole side chain of His 53 sits between the C-3′ and C-4′ oxygens, and the guanidinium group of Arg 97 lies within hydrogen bonding distance of the C-4′ keto oxygen.

A catalytic mechanism can thus be envisioned whereby His 51 abstracts the C-3′ proton leading to the formation of an enolate intermediate as indicated in Scheme 3. The side chain of Tyr 37 functions as an active site acid by protonating the C-4′ carbon, thereby leading to retention of the "glucose" configuration of the product. The role of His 53 is most likely to shuttle protons from the C-3′ hydroxyl to the C-4′ keto group (Fig. 5 and Scheme 3). Possible side chains that might stabilize the enolate intermediate include Arg 97 and/or Gln 58. Whereas Gln 58 is absolutely conserved amongst the 3,4-ketoisomerases, the equivalent position for Arg 97 is sometimes occupied by a histidine or a glycine residue.[12] The mechanism outlined in Scheme 3 is proposed as step wise, but it is also possible that proton transfer occurs in a concerted manner.

The 3,4-ketoisomerases are, indeed, an intriguing class of enzymes in that they utilize the same substrate, dTDP-4-keto-6-deoxyglucose, but some function as retaining enzymes such as QdtA or inverting enzymes such as FdtA (Scheme 2). An elegant biochemical investigation of another 3,4-ketoisomerase from *S. fradiae* suggested

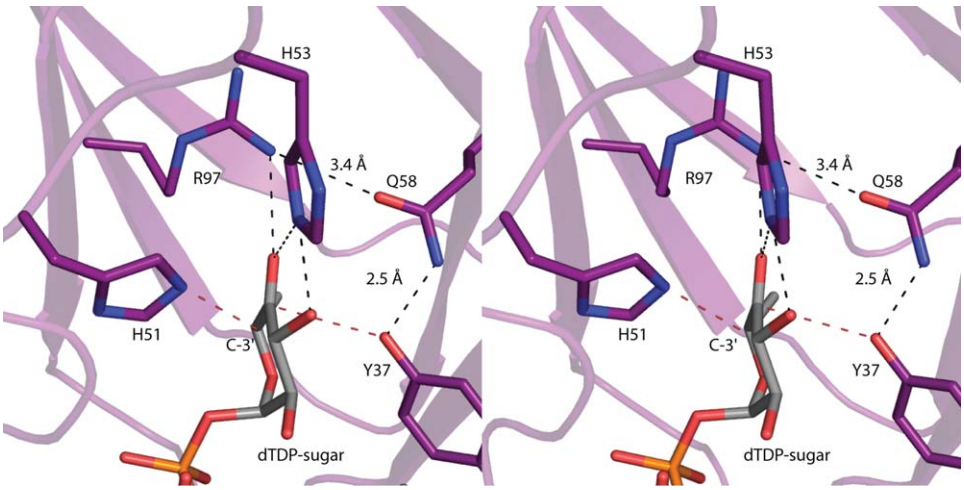

Figure 5. Model of the Michaelis Complex. In the complex, His 51 and Tyr 37 are located on opposite sides of the hexose moiety and are ideally positioned to serve as a catalytic base and acid, respectively (red dashed lines). There is a hydrogen-bonding network, indicated by the dashed black lines, between Arg 97, Gln 58, and Tyr 37. This may help to lower the pK_a of Tyr 37.

similar catalytic roles for His 63 (His 51 in QdtA) and Tyr 49 (Tyr 37 in QdtA), although there are no published crystal structures of this enzyme thus far. Like QdtA, the *S. fradiae* protein is a retaining enzyme.[13]

Very recently we reported a combined biochemical and structural investigation on the 3,4-ketoisomerase from *Shewanella denitrificans*. As observed for FdtA, this enzyme inverts the stereochemistry

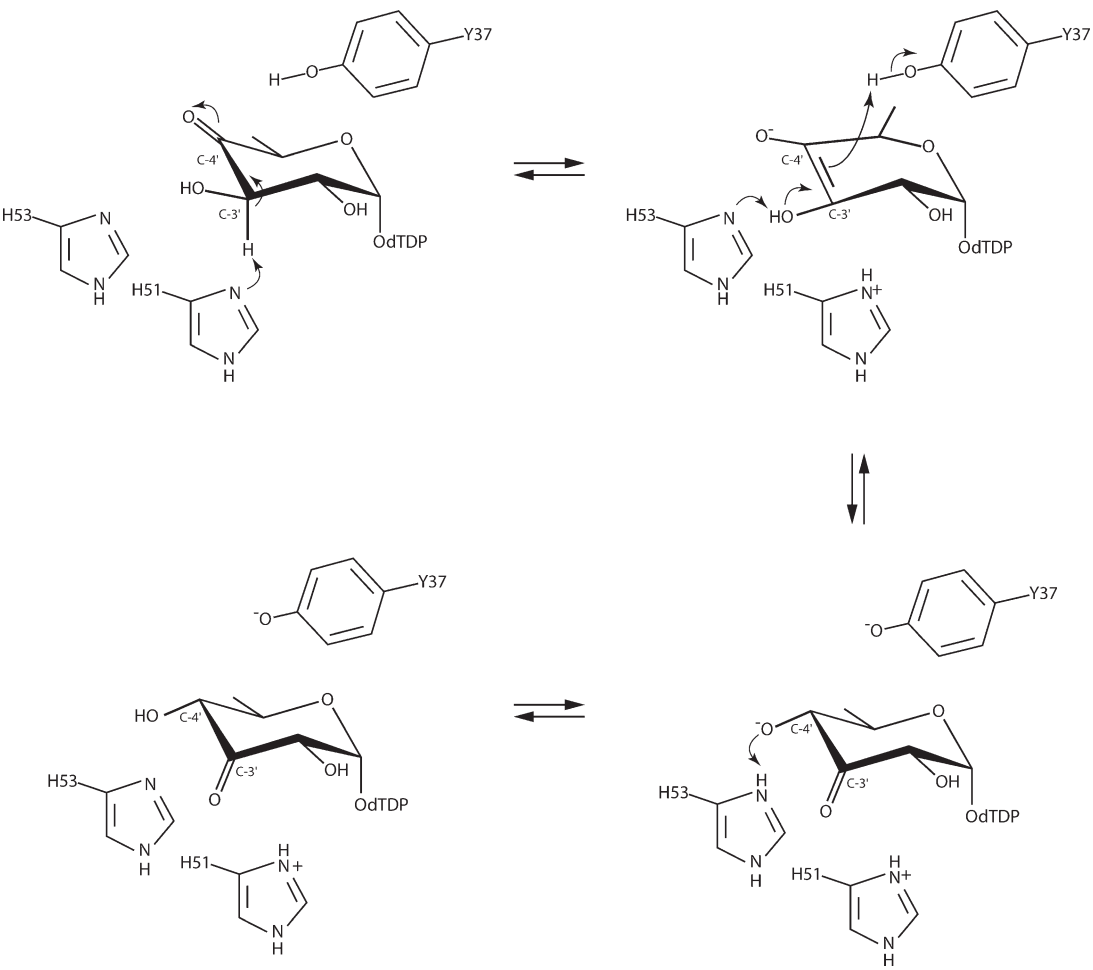

Scheme 3. Possible mechanism for QdtA.

Table I. *X-Ray Data Collection Statistics*

	QdtA with bound dTDP	QdtA H51N with bound dTDP-4-keto-6-deoxyglucose
Resolution limits	30–2.0 (2.05–2.0)[a]	50–1.90 (2.0–1.9)
Number of independent reflections	28,352 (2040)	33,577 (4259)
Completeness (%)	98.2 (97.9)	95.7 (87.1)
Redundancy	6.5 (5.1)	7.7 (2.1)
Avg I/avg $\sigma(I)$	18.5 (3.7)	14.9 (1.9)
R_{sym} (%)[b]	6.9 (28.2)	7.9 (37.4)

[a] Statistics for the highest resolution bin.
[b] $R_{sym} = (\Sigma | I - \bar{I} | / \Sigma I) \times 100$.

about the C-4′ carbon.[12] Importantly, whereas His 51 and His 53 are conserved in the *S. denitrificans* enzyme, Tyr 37 is replaced with a phenylalanine.[12] Based on amino acid sequence alignments of the 3,4-ketoisomerases, there is obviously a subset of these enzymes that contain a phenylalanine rather than a tyrosine residue in the active site. Thus a different mechanism must be operative in these inverting enzymes, most likely involving the two conserved histidines. Deprotonation of the C-3′ carbon and protonation of the C-4′ carbon on the same side of the pyranosyl ring would result in inversion of configuration.

Clearly, the *S. denitrificans* enzyme functions as an inverting enzyme because it lacks the required catalytic acid oriented on the opposite side of the pyranosyl ring. The reason why FdtA is an inverting enzyme is less clear, however. As in QdtA, it contains a tyrosine residue at Position 37 (Fig. 2). Indeed, the only significant difference between FdtA and QdtA is the replacement of Arg 97 in QdtA for a histidine residue in FdtA. Such a replacement could result in a charge change in the active site, thus dramatically affecting the pK_a of catalytically important residues and/or the manner in which the substrate binds. It could also affect a proton shuttling network. For example, in QdtA, Arg 97 is bridged to Tyr 37, the putative catalytic acid, via the side chain of Gln 58 (Fig. 5). In FdtA, this hydrogen-bonding network is broken, which may perturb the pK_a of the corresponding tyrosine enough that it can no longer function as a catalytic acid. Experiments designed to more fully explore the reaction mechanisms of the inverting and retaining 3,4-ketoisomerases are in progress.

Materials and Methods

Cloning of QdtA

The gene encoding QdtA was polymerase chain reaction (PCR)-amplified from *T. thermosaccharolyticum* E207-71 genomic DNA via standard procedures using primers such that the forward (5′-AAA*C*ATATGATTTTGTATAACGTT GCGTTAATAAA ATTTAAGGATATAGCAGATAAATATGGTCATTTGAC ACC) and the reverse (5′-AAA*CTCGAG*AAATCTTTT TTTAGCTTCATCAATATAAAA ATCATAATTTCTTAT GTAGTCCGTTTCATCAC) added NdeI and XhoI cloning sites, respectively. The purified PCR product was subsequently A-tailed and ligated into the pGEM-T vector (Promega), which was used to transform DH5-α *Escherichia coli* cells for subsequent screening and sequencing. A pGEM-T-*qdtA* vector construct of the correct sequence was digested and ligated into the pET31 vector for protein expression. DH5-α *E. coli* cells were transformed with the resulting plasmid and streaked onto lysogeny broth agar plates supplemented with ampicillin. Multiple colonies were tested for the presence of the *qdtA* gene.

Protein expression and purification

The purified pET31-*qdtA* plasmid was used to transform Rosetta (DE3) *E. coli* cells (Novagen). Cultures were grown in terrific broth medium supplemented with ampicillin and chloramphenicol at 37°C with shaking until an optical density of 0.9 was reached at 600 nm. The flasks were cooled to room temperature, and the cells were induced by the addition of 0.5 m*M* isopropyl-β-D-1-thiogalactopyranoside. They

Table II. *Refinement Statistics*

	QdtA with bound dTDP	QdtA H51N with bound dTDP-4-keto-6-deoxyglucose
Resolution limits (Å)	30.0–2.0	30–1.9
[a]R-Factor (overall)%/ no. reflections	19.9/28352	20.3/33577
R-Factor (working)%/ no. reflections	19.7/26835	20.1/31868
R-Factor (free)%/ no. reflections	23.9/1517	24.1/1709
Number of protein atoms	2283	2316
Number of heteroatoms	195	274
Average B values		
Protein atoms (Å^2)	36.1	27.8
Ligand (Å^2)	47.4	21.7
Solvent (Å^2)	42.1	57.8
Weighted RMS deviations from ideality		
Bond lengths (Å)	0.006	0.009
Bond angles (°)	2.4	1.4
Planar groups (Å)	0.012	0.006
Ramachandran regions (%)[b]		
Most favored	89.4	89.9
Additionally allowed	9.3	9.7
Generously allowed	1.2	0.4
Disallowed	0.0	0.0

[a] R-Factor $= (\Sigma | Fo - Fc | / \Sigma | Fo |) \times 100$ where Fo is the observed structure factor amplitude and Fc is the calculated structure factor amplitude.
[b] Distribution of Ramachandran angles according to PROCHECK.[20]

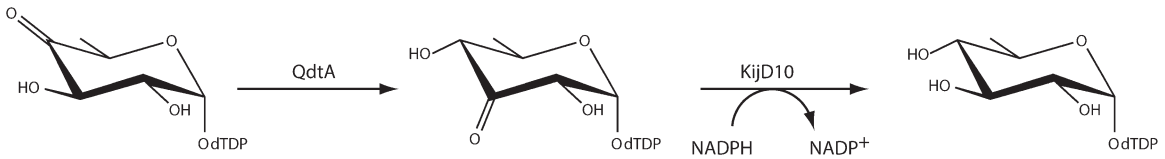

Scheme 4. Coupled assay used to measure QdtA activity.

were allowed to express protein at 23°C for 24 h following induction.

The cells were harvested by centrifugation and disrupted by sonication on ice. The lysate was cleared by centrifugation, and QdtA was purified utilizing Ni nitrilotriacetic acid resin (Qiagen) according to the manufacturer's instructions. The protein was dialyzed against 10 m*M* Tris–HCl (pH 8.0) and 200 m*M* NaCl and concentrated to 20 mg mL^{-1} based on an extinction coefficient of 0.77 mg^{-1} mL cm^{-1}.

Preparation of dTDP-4-keto-6-deoxyglucose

dTDP-4-keto-6-deoxyglucose was prepared by dissolving dTDP–glucose in 1 mL of 50 m*M* *N*-2-hydroxyethylpiperazine-*N*′-3-propanesulfonic acid (HEPPS; pH 8.5) containing 10 mg of *E. coli* RmlB (4,6-dehydratase) to a final concentration of 50 m*M*. This reaction was incubated at 37°C for 6 h. The resulting dTDP-4-keto-6-deoxyglucose was used without further purification. Note that high-performance liquid chromatography (HPLC) analysis of the mixture at this time point showed that the reaction was essentially complete and negligible amounts of dTDP–glucose were present. RmlB was purified in the laboratory as a C-terminal His_6 construct (unpublished procedures).

Crystallization of QdtA

Prior to crystallization trials, the protein was incubated with 10 m*M* dTDP. Crystallization conditions were then surveyed by the hanging drop method of vapor diffusion using a sparse matrix screen developed in the laboratory. Single crystals of QdtA were subsequently grown against a precipitant solution containing 100 m*M* HEPPS (pH 8.0) and 22–28% pentaerythritol propoxylate. The crystals belonged to the space group $P42_12$ with unit cell dimensions of $a = b = 95.8$ Å and $c = 94.7$ Å. The asymmetric unit contained one dimer.

Site-directed mutagenesis and crystallization

The site-directed mutant protein, H51N, was generated using the QuikChange method of Stratagene. The protein variant was expressed and purified as described above for the wild-type enzyme.

Crystals were grown under conditions similar to that of the wild-type enzyme, except that no ligands were included in the experiments. The ligand-free crystals were transferred to a synthetic mother liquor containing 30% pentaerythritol propoxylate, 200 m*M* NaCl, 100 m*M* HEPPS (pH 8.0), and 10 m*M* dTDP-4-keto-6-deoxyglucose. They were allowed to soak for 18 h.

Structural analysis of QdtA

Prior to X-ray data collection, crystals of the wild-type enzyme were transferred to a cryoprotectant solution containing 32% pentaerythritol propoxylate, 200 m*M* NaCl, 10 m*M* dTDP, and 100 m*M* HEPPS (pH 8.0). X-ray data were collected at 100 K with a Bruker AXS Platinum 135 CCD detector controlled by the Proteum software suite (Bruker AXS). The X-ray source was Cu Kα radiation from a Rigaku RU200 X-ray generator equipped with Montel optics and operated at 50 kV and 90 mA. These X-ray data were processed with SAINT version 7.06A (Bruker AXS) and internally scaled with SADABS version 2005/1 (Bruker AXS). Relevant X-ray data collection statistics are listed in Table I. The structure was solved with PHASER using the coordinates for FdtA (PDB code 2PA7) as a search model.[8,14] Iterative rounds of model building with COOT and refinement with REFMAC reduced the R_{work} and R_{free} to 19.7 and 23.9%, respectively, from 30 to 2.0 Å resolution.[15,16]

Crystals of the H51N variant were transferred to a cryoprotectant solution containing 36% pentaerythritol propoxylate, 200 m*M* NaCl, 6% ethylene glycol, 10 m*M* dTDP-4-keto-6-deoxyglucose, and 100 m*M* HEPPS (pH 8.0). X-ray data were collected and processed in a similar manner as that described above for the wild-type enzyme. Relevant statistics are presented in Table I. Iterative cycles of model-building with COOT and refinement with REFMAC reduced the R_{work} and R_{free} to 20.1 and 24.1%, respectively, from 30 to 1.90 Å resolution.[15,16] Model refinement statistics are listed in Table II for both the wild-type enzyme and the H51N mutant protein.

QdtA activity

The 3,4-ketoisomerase activity of QdtA was verified via a coupled assay. Specifically, a 1.0 mL reaction mixture was set up that contained 1 m*M* dTDP–glucose, 2 mg mL^{-1} of *E. coli* RmlB, 1 mg mL^{-1} QdtA, 4 mg mL^{-1} *T. thermosaccharolyticum* QdtB, 40 m*M* sodium glutamate, and 100 m*M* HEPPS (pH 8). The functions of RmlB and QdtB are shown in Scheme 2. The reaction was incubated at 37°C for 2 h. Enzymes were removed, and the reaction products

were evaluated via HPLC. The amino sugar product had the same retention time as that of a standard dTDP-3-amino-6-deoxyglucose sample. QdtB was purified as previously described.[17]

Kinetic analysis

The kinetic constants for the 3,4-ketoisomerase reaction were determined via a coupled assay using a Beckman Coulter DU-640 spectrophotometer according to Scheme 4. The activity of QdtA was measured by monitoring the decrease in absorbance at 340 nm as NADPH is oxidized to $NADP^+$ due to the action of KijD10. Previous studies from the laboratory have verified that KijD10 from *Actinomadura kijaniata* functions as an NADPH-dependent C-3′ ketoreductase.[18] The reaction mixtures contained 50 m*M* HEPES (pH 7.5), 0.2 m*M* NADPH, 1 mg mL^{-1} KijD10, and dTDP-4-keto-6-deoxyglucose varying from 0.025 to 5.0 m*M*. The reactions were performed at 23°C and initiated by the addition of 0.005 mg mL^{-1} QdtA. No measurable activity was observed for the H51N mutant protein.

Sequencing data

The amino acid sequence of QdtA from *T. thermosaccharolyticum* was deposited into GenBank (AAR85518.1) in 2008. Surprisingly, our multiple and independent PCRs using Platinum *Pfx* polymerase always showed the following four amino acid substitutions in the PCR products: A52S, F94L, L95V, and C116Y. To verify that these variations from the published sequence were correct and not a function of the polymerase, PCRs were subsequently performed using *PfuTurbo* DNA Polymerase (Stratagene). The resulting products also contained the same changes from the deposited sequence.

Acknowledgment

The authors thank Professor Grover L. Waldrop for helpful discussions.

References

1. Pfoestl A, Hofinger A, Kosma P, Messner P (2003) Biosynthesis of dTDP-3-acetamido-3,6-dideoxy-alpha-D-galactose in *Aneurinibacillus thermoaerophilus* L420-91T. J Biol Chem 278:26410–26417.
2. Pfostl A, Zayni S, Hofinger A, Kosma P, Schaffer C, Messner P (2008) Biosynthesis of dTDP-3-acetamido-3,6-dideoxy-alpha-D-glucose. Biochem J 410:187–194.
3. Aspinall GO, McDonald AG, Pang H, Kurjanczyk LA, Penner JL (1993) Lipopolysaccharide of *Campylobacter coli* serotype O:30. Fractionation and structure of liberated core oligosaccharide. J Biol Chem 268:6263–6268.
4. Perry MB, MacLean LL (1999) Structural characterization of the antigenic O-chain of the lipopolysaccharide of *Escherichia coli* serotype O65. Carbohydr Res 322: 57–66.
5. Kocharova NA, Blaszczyk A, Zatonsky GV, Torzewska A, Bystrova OV, Shashkov AS, Knirel YA, Rozalski A (2004) Structure and cross-reactivity of the O-antigen of *Providencia stuartii* O18 containing 3-acetamido-3,6-dideoxy-D-glucose. Carbohydr Res 339:409–413.
6. Zych K, Perepelov AV, Siwinska M, Knirel YA, Sidorczyk Z (2005) Structures of the O-polysaccharides and classification of *Proteus* genomospecies 4, 5 and 6 into respective *Proteus* serogroups. FEBS J 272:5536–5543.
7. Bryskier AJ (1993) Macrolides: chemistry, pharmacology, and clinical uses. Paris: Arnette Blackwell.
8. Davis ML, Thoden JB, Holden HM (2007) The X-ray structure of dTDP-4-keto-6-deoxy-D-glucose-3,4-ketoisomerase. J Biol Chem 282:19227–19236.
9. Dunwell JM, Culham A, Carter CE, Sosa-Aguirre CR, Goodenough PW (2001) Evolution of functional diversity in the cupin superfamily. Trends Biochem Sci 26:740–746.
10. Dunwell JM, Purvis A, Khuri S (2004) Cupins: the most functionally diverse protein superfamily? Phytochemistry 65:7–17.
11. Galperin MY, Koonin EV (2012) Divergence and convergence in enzyme evolution. J Biol Chem 287:21–28.
12. Chantigian DP, Thoden JB, Holden HM (2013) Structural and biochemical characterization of a bifunctional ketoisomerase/*N*-acetyltransferase from *Shewanella denitrificans*. Biochemistry 52:8374–8385.
13. Tello M, Rejzek M, Wilkinson B, Lawson DM, Field RA (2008) Tyl1a, a TDP-6-deoxy-D-xylo-4-hexulose 3,4-isomerase from *Streptomyces fradiae*: structure prediction, mutagenesis and solvent isotope incorporation experiments to investigate reaction mechanism. Chembiochem 9:1295–1302.
14. McCoy AJ, Grosse-Kunstleve RW, Adams PD, Winn MD, Storoni LC, Read RJ (2007) Phaser crystallographic software. J Appl Cryst 40:658–674.
15. Emsley P, Cowtan K (2004) Coot: model-building tools for molecular graphics. Acta Crystallogr D Biol Crystallogr 60:2126–2132.
16. Murshudov GN, Vagin AA, Dodson EJ (1997) Refinement of macromolecular structures by the maximum-likelihood method. Acta Crystallogr D Biol Crystallogr 53:240–255.
17. Thoden JB, Schaffer C, Messner P, Holden HM (2009) Structural analysis of QdtB, an aminotransferase required for the biosynthesis of dTDP-3-acetamido-3,6-dideoxy-alpha-D-glucose. Biochemistry 48:1553–1561.
18. Kubiak RL, Holden HM (2011) Combined structural and functional investigation of a C-3″-ketoreductase involved in the biosynthesis of dTDP-L-digitoxose. Biochemistry 50:5905–5917.
19. DeLano WL (2002) The PyMOL Molecular Graphics System. San Carlos, CA: DeLano Scientific.
20. Laskowski RA, Moss DS, Thornton JM (1993) Main-chain bond lengths and bond angles in protein structures. J Mol Biol 231:1049–1067.